Human iPSC-Derived Posterior Gut Progenitors Are Expandable and Capable of Forming Gut and Liver Organoids

Ran-Ran Zhang,[1,2] Masaru Koido,[1] Tomomi Tadokoro,[1] Rie Ouchi,[2] Tatsuya Matsuno,[1] Yasuharu Ueno,[1] Keisuke Sekine,[1] Takanori Takebe,[1,2,3,4,5,6,*] and Hideki Taniguchi[1,2,6,*]

[1]Department of Regenerative Medicine, Yokohama City University Graduate School of Medicine, Kanazawa-ku 3-9, Yokohama, Kanagawa 236-0004, Japan
[2]Division of Gastroenterology, Hepatology & Nutrition, Developmental Biology, Center for Stem Cell and Organoid Medicine (CuSTOM), Cincinnati Children's Hospital Medical Center, Cincinnati, OH 45229-3039, USA
[3]Advanced Medical Research Center, Yokohama City University, Kanazawa-ku 3-9, Yokohama, Kanagawa 236-0004, Japan
[4]PRESTO, Japan Science and Technology Agency, 4-1-8 Honcho, Kawaguchi, Saitama 332-0012, Japan
[5]Department of Pediatrics, University of Cincinnati College of Medicine, Cincinnati, OH, USA
[6]Co-senior author
*Correspondence: takanori.takebe@cchmc.org (T.T.), rtanigu@yokohama-cu.ac.jp (H.T.)
 https://doi.org/10.1016/j.stemcr.2018.01.006

SUMMARY

Early endoderm progenitors naturally possess robust propagating potential to develop a majority of meter-long gastrointestinal tracts and are therefore considered as a promising source for therapy. Here, we demonstrated the reproducible generation of human CDX2^{+} posterior gut endoderm cells (PGECs) from five induced pluripotent stem cell clones by manipulating *FGF*, *TGF*, and *WNT* signaling. Transcriptome analysis suggested that putative PGECs harbored an intermediate signature profile between definitive endoderm and organ-specific endoderm. We found that combinatorial EGF, VEGF, FGF2, Chir99021, and A83-01 treatments selectively amplify storable PGECs up to 10^{21} cell scale without any gene transduction or feeder use. PGECs, compared with induced pluripotent stem cells, showed stable differentiation propensity into multiple endodermal lineages without teratoma formation. Furthermore, transplantation of PGEC-derived liver bud organoids showed therapeutic potential against fulminant liver failure. Together, the robustly amplified PGECs may be a promising cellular source for endoderm-derived organoids in studying human development, modeling disease, and, ultimately, therapy.

INTRODUCTION

Targeting Developmental Progenitors for Future Applications

Transient amplification of developmental progenitors during early organogenesis is a mechanism for ensuring organ growth. These progenitor cells are amenable to proliferative stimuli because of their high levels of both genomic and epigenetic stability (Cang et al., 2007; Elliott et al., 2015; Shi et al., 2013). Although pluripotent stem cells (PSCs) show unlimited capacity for *in vitro* expansion, recent emerging evidence suggests that factors including genetic and epigenetic variations or chromosomal instabilities (Peterson and Loring, 2014) may change the properties of PSCs and their derivations, thus dampening their utility for future applications, because of the resulting high risk of tumorigenicity (Lund et al., 2012). Therefore, targeting such developmental progenitors seems to be a reasonable strategy to obtain a large number of cells for subsequent application purposes. Although some attempts have been made to differentiate cardiac (Christoforou et al., 2013; Wang et al., 2013), endodermal (Cheng et al., 2012; Hannan et al., 2013), renal (Hu et al., 2010), neuronal, and cortical (Hu et al., 2010; Shi et al., 2012) progenitors by using pluripotency, establishing a stable source of developmental progenitors remains a challenge.

Developmental Gut Progenitors in the Posterior Region

Human posterior gut endodermal progenitors, herein referred to as PGECs, are found along almost the entire length of the gut (Franklin et al., 2008) and eventually develop the majority of the gastrointestinal (GI) tract (Sheaffer and Kaestner, 2012), which is approximately 9 m in length (including approximately 6 m of small intestine and 3 m of colon) (Tortora and Derrickson, 2008). Indeed, the total number of epithelial cells composing the GI tract is not known. It has been estimated that there are 5×10^{10} human colonic epithelial cells in the gut and that 20% of them are replaced each day (Hagedorn et al., 2011), indicating the high expansion capability of PGECs.

Posterior gut specification occurs at a caudal part of the primitive gut endoderm on embryonic day 8.5 (E8.5) in mice and day 20 in human stem cell culture (McCracken et al., 2014), and this process primarily contributes to the formation of the small and large intestines in adults (Wells and Melton, 1999). Relative to the anterior domain of the endoderm, posterior gut progenitors elongate, forming a significantly longer segment of the gut through extensive proliferation and migration (Franklin et al., 2008). It is likely that PGEC rearrangement and proliferation are required to achieve the expansion of the gut endoderm. One current major unmet challenge involves the

recapitulation of the differentiation process of PGECs in a dish from pluripotent cells.

Molecular Identity of the CDX2-Positive Posterior Gut Endoderm

Previous fate-mapping studies have revealed the complex genetic program involving anterior-posterior patterning of embryonic gut tubes derived from definitive endoderm cells (Ikonomou and Kotton, 2015; Sherwood et al., 2009). The regional identify of the developing gut tube is specifically separated by *Sox2* and *Cdx2*, i.e., an anterior *Sox2*^{+} domain and a posterior caudal-related homeobox transcription factor (*Cdx2*)[+] domain (Ikonomou and Kotton, 2015). From mouse E8.5 onward, *Cdx2* is predominantly activated in the posterior part of gut. Subsequently, *Cdx2* expression is restricted to the intestinal epithelium posterior to the transition from the stomach to the duodenum (Sherwood et al., 2009). Genetic and functional analyses of the posterior endoderm marker *Cdx2* have revealed that conditional ablation of *Cdx2* results in expansion of the anterior foregut, as indicated by ectopic *Sox2* expression (Ikonomou and Kotton, 2015). Additionally, a *Cdx2*-deficient gut converts the colon into a proximal intestinal identity whereas ectopic expression of *Cdx2* in gastric epithelial cells induces intestinal metaplasia, an example of a posterior homeotic transformation (Silberg et al., 2002).

WNT-Based Gut Specification and Extension of the CDX2-Positive Posterior Gut

Previous studies have shown that multiple signaling pathways converge on *Cdx2* and mediate endoderm posteriorization, such as Wnt (Sherwood et al., 2011) and fibroblast growth factor (*FGF*) signaling (Chawengsaksophak et al., 2004). Genetic activation of the Wnt pathway directly on the endoderm induces *Cdx2* expression with a shifting phenotype from anterior endoderm to posterior endoderm (Sherwood et al., 2011). Additionally, chemical activation of Wnt signaling efficiently induces *Cdx2* expression by suppressing anterior foregut fates (Ikonomou and Kotton, 2015). *Wnt3a*-null mutants exhibit a posterior-truncated phenotype similar to that of *Cdx2*-null embryos (Chawengsaksophak et al., 2004), and partial ablation of Wnt signaling in *Wnt5a*-null mice results in a dramatically shortened small intestine (Cervantes et al., 2009), with a phenotype similar to that of the *Cdx2* mutant gut (Gao et al., 2009). In addition, FGF signaling plays an essential role in determining the *Sox2-Cdx2* boundary at the duodenal-pyloric junction (Sheaffer and Kaestner, 2012).

Canonical Wnt signaling (Gregorieff and Clevers, 2005) and the inhibition of transforming growth factor β (TGF-β) signaling promote human colonic crypt stem/progenitor cell (Reynolds et al., 2014). Additionally, mini-gut organoids require epidermal growth factor (EGF) signal activation for long-term culture (Date and Sato, 2015). In zebrafish, vascular endothelial growth factor (VEGF) is required for early gut-tube morphogenesis (Zorn and Wells, 2009). Both FGF and Wnt signaling are required for posterior gut endoderm marker *Cdx2* expression (Sherwood et al., 2011). The current study seeks to differentiate human induced PSCs (iPSCs) into CDX2-positive (CDX2^{+}) human posterior gut progenitors and amplify this CDX2^{+} population by recapitulating early endoderm organogenesis. We also investigated the self-organizing potential of these cells to develop into liver bud organoids as well as two endoderm derivatives including hepatic and hindgut lineages, with the aim of applying these cells for future therapeutic use.

RESULTS

Derivation of Expandable CDX2^{+} Posterior Gut Endoderm Cells from Human iPSCs by Using a Combination of Five Factors

We used a specified stepwise differentiation protocol in serum-free medium (SFD) that has previously been shown (Gouon-Evans et al., 2006) to induce definitive endoderm (DE) (Figure S1A) cell fate in multiple human iPSC lines (TKDA3-4, and four xeno-free iPSCs 1231A3, 1383D2, 1383D6, and Ff06). Four of the iPSCs were cultured on Laminin-511 E8 fragment (iMatrix)-coated dishes, whereas TKDA3-4 iPSC and its derivatives were cultured on Matrigel-coated dishes. This DE induction protocol mimics embryogenesis by initial treatment with activin A and Wnt3a for 2 days, followed by bone morphogenetic protein 4 (BMP4), FGF2, VEGF, and activin A treatment for 4 days. The generated DE cells were subsequently replated onto Matrigel- or Laminin-511 E8-coated culture dishes at a 1:1 ratio to specify PGECs (Figure 1A). In the mouse early embryo, *Cdx2* is activated and predominantly expressed in the posterior gut (Hannan et al., 2013). Therefore, we first performed screening experiments to initiate expression of the posterior gut endoderm marker *CDX2* in cells induced with different combinations of various potential inducers, based on gene expression profiling using qRT-PCR (Figure 1B). In contrast to the endodermal progenitor derivation protocol (Cheng et al., 2012), BMP4 could not induce high *CDX2* expression and DE cells were efficiently converted into *CDX2*-positive PGECs in the presence of three factors: the growth factor FGF2 and the small molecules Chir99021 and A83-01. Interestingly, after only 1 day of induction, these cultured cells exhibited morphology distinct from that of DE cells (Figure 1C). However, treatment with only FGF2 or Chir99021 and A83-01 failed to induce *CDX2* expression, whereas the combination of
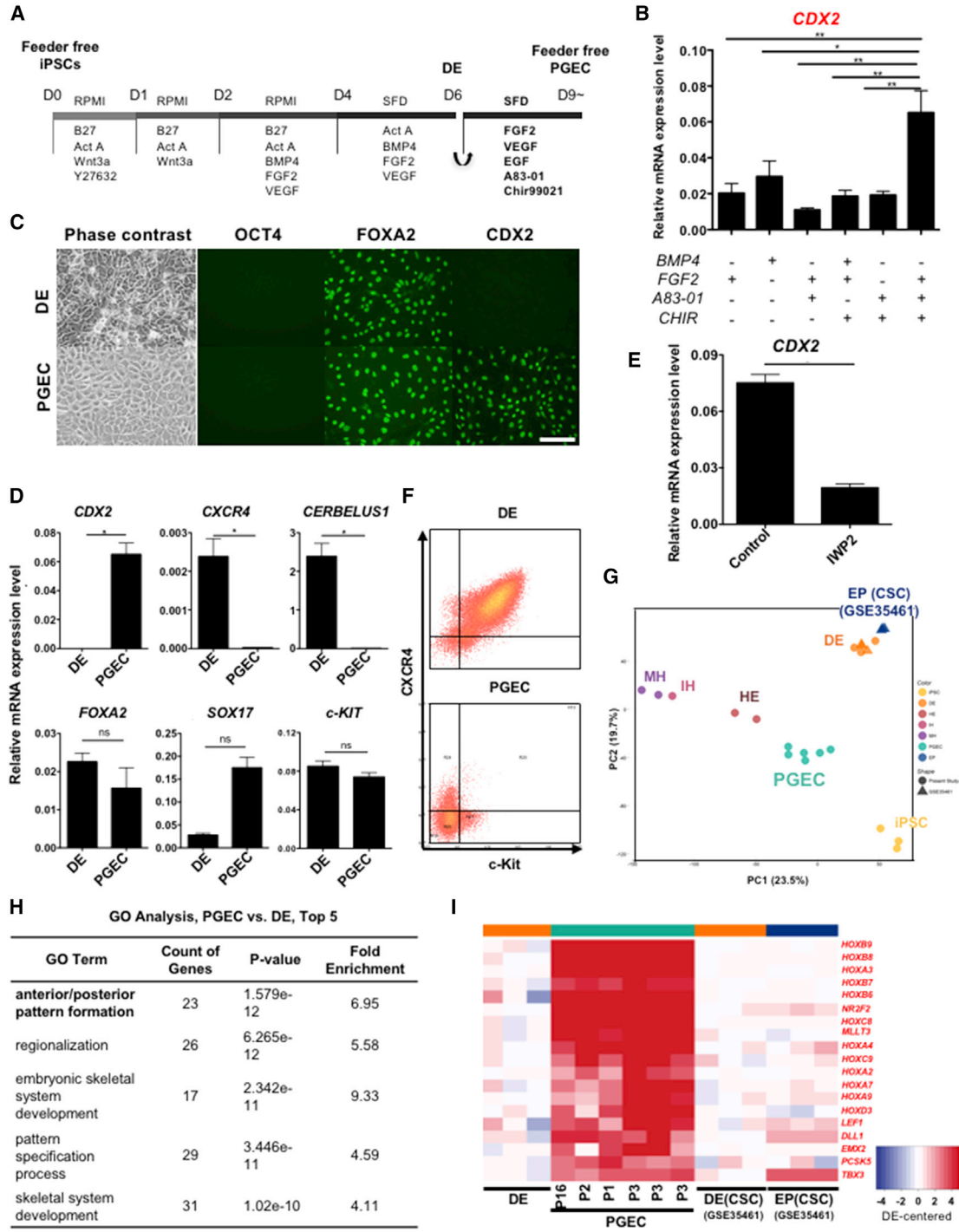
Figure 1. Directed Differentiation into CDX2+ Posterior Gut Endoderm Progenitor Cells

(A) Schematic of human iPSC-derived PGEC differentiation protocol in medium containing Chir99021 (CHIR), A83-01, epidermal growth factor (EGF), basic growth factor 2 (FGF2), and vascular endothelial growth factor (VEGF). PGEC, posterior gut endoderm cells.

(B) Effect of *CDX2* gene expression induction under indicated media treatment (n = 3 independent experiments, mean ± SEM; *p < 0.05, **p < 0.01).

(C) Phase-contrast image shows the morphology of differentiated DE and TKDA3-4 iPSC induced PGECs after initial passage; immunostainings show expression of OCT4, FOXA2, and CDX2. Scale bar, 100 μm.

(legend continued on next page)

those three factors generated *CDX2*-positive PGECs (Figure 1B). Immunostaining revealed that the endoderm cell marker *FOXA2* was present in both DE cells and PGECs, whereas *CDX2* was specifically expressed in PGECs (Figure 1C). qPCR analysis further revealed low expression of the DE cell-specific markers *CXCR4* and *CERBELUS1* and high expression posterior gut marker *CDX2* as well as a similar expression level of endodermal marker *FOXA2* and *SOX17* in PGECs compared with DE (Figure 1D). Additionally, inhibition of the WNT signaling pathway by using IWP2 significantly downregulated posterior gut-related marker *CDX2* expression (Figure 1E), while no significant effect was detect on the expression of DE-related marker *FOXA2*, *SOX17*, and *CXCR4* in PGECs (Figure S2B), thus suggesting an important role of the Wnt pathway for posterior gut induction, in agreement with previously published data (Gao et al., 2009). To confirm whether PGECs were contaminated with DE cells, we used flow cytometry to analyze the DE cell markers CXCR4 and c-KIT. We found that the CXCR4$^+$c-KIT$^+$ population was broadly present among DE cells, whereas almost no CXCR4$^+$c-KIT$^+$ DE cells were detected in PGECs (Figures 1F and S1B).

Furthermore, principal component analysis (PCA) based on global transcriptomic data revealed that PGECs derived from different iPSC clones (TKDA3-4, Ff06, 1231A3, and 1383D6) exhibited a unique intermediate state of lineage among DE cells and hepatic endoderm (HE) (Figure 1G). Notably, based on PCA of gene expression profiles, the cellular identity of PGECs was significantly different from that of previously published endodermal progenitor (EP) cells, based on publicly available expression data (Cheng et al., 2012) (Figure 1G). An unbiased functional enrichment analysis of gene ontology (GO) terms showed that the general categories of biological processes including anterior/posterior (A-P) pattern formation and regionalization were significantly enriched in PGEC-upregulated genes compared with DE cells (Figure 1H). In a number of non-endoderm tissues, *Cdx* factors exert their developmental effects by regulating *Hox* transcription factors,

which are critical for the A-P patterning process of the vertebrate embryo (Gao et al., 2009). Interestingly, PGECs exhibited posterior properties by strongly expressing *CDX2* with a number of posterior *HOX* genes, including *HOXC8*, *HOXB9*, and *HOXC9*, while still maintaining anterior properties, as evidenced by *HOXA3* expression, thus suggesting that iPSC derived PGECs possess a previously undescribed A-P transitional phenotype with posterior gut identity (Figure 1I).

Characterization of Extensively Propagated PGECs

Next, we sought to determine whether the modified culture medium could sustain the expansion of PGECs. As an initial screen, we passaged PGECs in the absence of each gut extension factor: EGF, VEGF, FGF2, Chir99021, A83-01, and Y27632. Among these factors, VEGF removal significantly abrogated the PGEC expansion capability, whereas removal of the other factors inhibited proliferation to a lesser extent (Figures 2A and S2A). Furthermore, inhibition of the *WNT* signaling pathway by using IWP2 significantly slowed PGEC expansion (Figure S2C). Four different donor-derived iPSC clone-derived PGECs were maintained (for approximately 1,015-, 1,019-, 1,019- and 1,020-fold expansion for up to 70 days of TKDA3-4, Ff06, 1231A3, and 1383D6 iPSC clone-derived PGECs, with doubling times of 33.09 hr, 21.65 hr, 23.13 hr, and 22.65 hr, respectively) for more than 20 passages and demonstrated epithelial-like morphology and proliferation (Figures 2B, S3A, and S3B). Over a number of passages, serial qRT-PCR (Figure 2D) and immunostaining analyses (Figures 2E and 2F) showed that the posterior gut phenotype was maintained with stable CDX2, SOX17, FOXA2, and c-KIT expression, and the cell proliferative capability was maintained with active Ki-67 expression (Figures 2E and 2F). Of note, the generation of PGECs from Ff06 iPSCs was carried out exclusively on Laminin-511 E8-coated dishes, and the resulting xeno-free PGECs also showed the same proliferative phenotype (Figure S3C). We then seeded the PGECs at a low density and followed them via

(D) Inhibitory effect of *CDX2* induction in PGECs in the presence of WNT signal pathway inhibitor IWP2 (n = 3 independent experiments, mean ± SEM; *p < 0.05).

(E) qRT-PCR of endoderm related gene expression in PGECs relative to DE. The definitive endoderm-specific gene *CXCR4/CERBELUS* and endodermal related gene *FOXA2/SOX17* as well as posterior gut-specific gene *CDX2* (n = 3 independent experiments, mean ± SEM; ns, no significant difference; *p < 0.05).

(F) Flow-cytometry analysis of the endoderm progenitor CXCR4/c-KIT double-positive cells in differentiated DE and PGECs. Representative data are shown from three separate experiments.

(G) PCA using our data (iPSC, DE, HE, IH, MH, and PGEC) and publicly available EP data (from GEO: GSE35461 [Gadue et al., 2013]) revealed the differential unique identity of PGECs. The variance of each PC is shown in each axis legend.

(H) GO analysis of differentially expressed genes (DEG) of PGECs, compared with DE. The top 5 significantly enriched terms are displayed.

(I) The heatmap of anterior/posterior pattern formation genes (GO:0009952, anterior/posterior pattern formation; DAVID Bioinformatics Resources 6.7) in DEG of PGECs were extremely highly expressed in PGECs and not in EP.
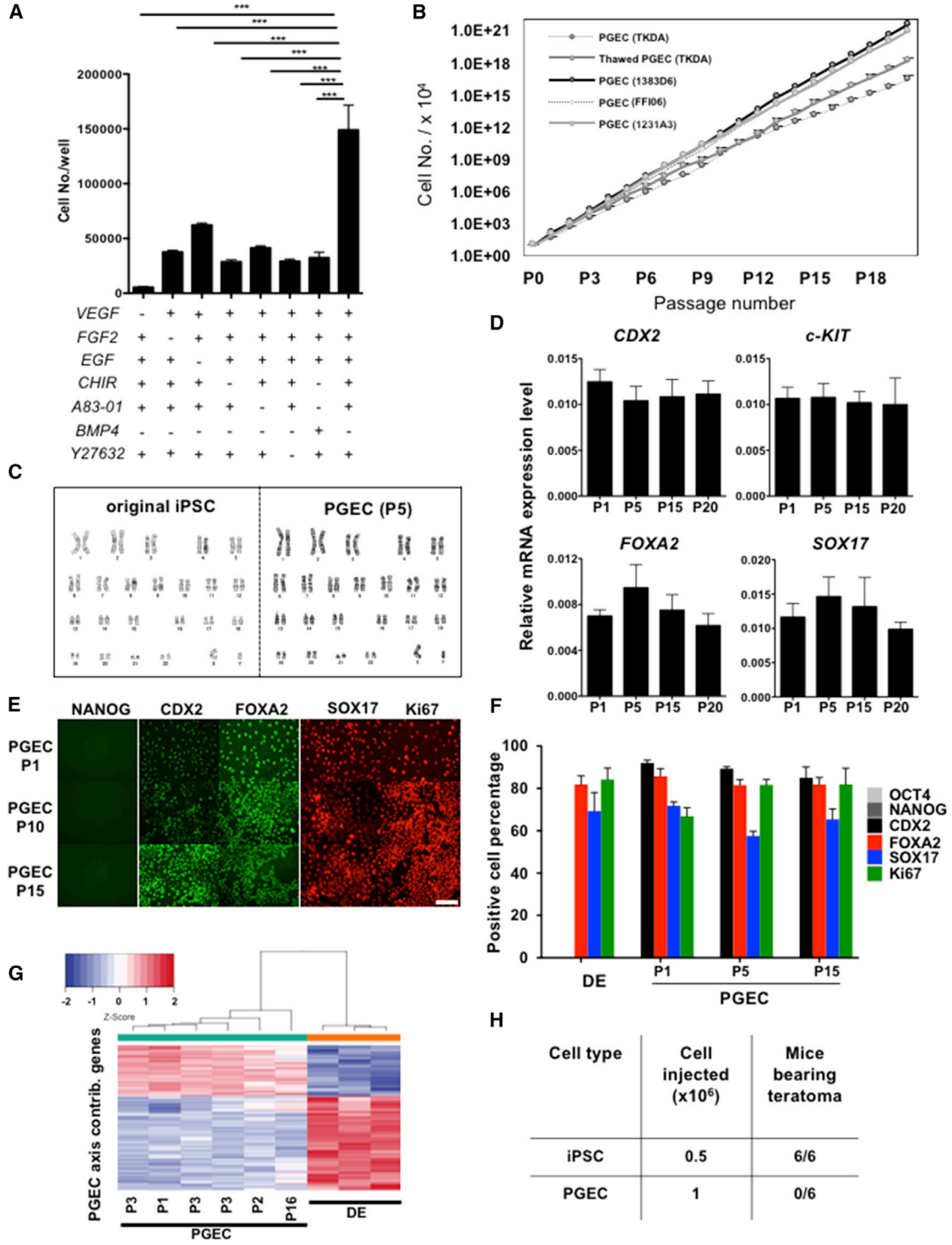
See also Figures S1 and S2.

Figure 2. Robust Propagation of CDX2⁺ Posterior Gut Endoderm Progenitor Cells

(A) Factor screening based on subsequent proliferative potential. The PGEC expansion cell number is quantified under treatment with a different combination of factors (n = 3 independent experiments, mean ± SEM; ***p < 0.001).

(B) Growth curve of PGECs derived from different iPSC clones (TKDA3-4, 1383D6, 1231A3, and Ff06) as well as frozen PGECs derived from TKDA3-4. PGECs derived from TKDA3-4, 1383D6, and 1231A3 are cultured under Matrigel coating, while Ff06-derived PGECs are cultured under Laminin coating (TKDA3-4, n = 3 independent experiments, mean ± SEM; 1383D6, 1231A3, Ff06, n = 1 independent experiment).

(legend continued on next page)

time-lapse microscopy. The results showed that the majority of cells were able to clonally propagate and form colonies within 4–5 days (Figures S3D and S3E), and expressed posterior gut endoderm markers (Figure S3F). Flow-cytometry analysis of PGECs showed that PGECs were negative for pluripotent-, mesenchyme-, endothelial-, and mesoderm-lineage markers (Figure S4B). Next, we conducted PCA using iPSC, DE, HE, immature hepatocyte (IH), mature hepatocyte (MH), and PGEC, and identified principal component 3 (PC3) as the PGEC axis (Figure S4C), which specifically divided PGECs and DE cells. Notably, PC3-contributed genes characterized PGECs and did not differentiate PGECs according to the number of passages (Figure 2G).

To determine chromosomal stability, we performed a karyotype analysis. PGECs passaged five times had one copy each of 23 chromosomes, similar to the normal original iPSC clone in the absence of monosomy or trisomy (Figure 2C). iPSCs possess a tumor-prone phenotype, which represents a major impediment for future clinical applications. To determine whether PGECs possess tumor-forming potential, we intracapsularly transplanted 1 million PGECs into the kidneys of NOD/SCID mice (Figure S5A). After 1 month of injection, six of the human iPSC-injected mice developed teratomas, whereas all six mice that received PGECs did not (Figure 2H). Next, we used immunohistochemistry to examine the tissues for endoderm formation potential. The generated tissue contained a structure resembling the hindgut epithelium and expressed the transcription factors CDX2 and SOX9 (Figure S5B) as well as pancreatic differentiation potentials with positively detected human PDX1 (Figure S5C). Together, these results demonstrated the reproducible generation of unique CDX2$^+$ PGECs with rigorous amplification and multi-differentiation potential from feeder-free human iPSCs.

PGECs Exhibited Potential of Developing Hindgut Organoids *In Vitro*

Following modification of a previously defined stepwise directed differentiation approach (Sato and Clevers, 2013) that mimics signaling events occurring during normal hindgut development *in vivo* (Figure 3A), we were able to promote cell differentiation *in vitro*. Remarkably, Chir99021- and FGF4-treated single PGEC suspensions underwent morphogenesis that was similar to embryonic hindgut formation. After 3 days of Chir99021 + FGF4 pre-treatment, two-dimensional (2D) cultured cell sheets started budding off and formed floating hindgut spheroids (Figure 3B). *In vitro* hindgut spheroid formation was never observed without Chir99021 + FGF4 treatment. These results support a previously described mechanism for gut development, whereby synergy between WNT signaling and FGF signaling is required for generation of the hindgut lineage.

We next investigated whether the spheroids could develop and differentiate into hindgut organoids *in vitro* by using three-dimensional (3D) culture conditions under published protocols. After the spheroids were embedded and after 7 days of culture, the epithelium of the spheroid differentiated and protruded into the lumen of the organoid when cells were pre-treated with Chir99021 + FGF4 (Figure 3C). PGEC-derived hindgut organoids comprise a mostly polarized epithelium that includes different differentiated cell types, confirmed by immunofluorescence and qPCR analysis. After 7 days in 3D culture, absorptive enterocytes (VILLIN$^+$) and hindgut epithelial cells (E-CAD$^+$) were both readily detected (Figures 3D and 3E). The hindgut transcription factors *CDX2* and *SOX9* were broadly detected, suggesting that the PGEC-derived spheroids embedded onto the matrix retain a hindgut phenotype. Thus, directed differentiation of PGECs into hindgut organoids could be achieved *in vitro*.

Hepatic Differentiation Potential Is Preferentially Induced in CDX2$^+$ PGECs

Experimental animal models have shown that the early endoderm or gut possesses relative plasticity for anterior versus posterior gut endoderm, and our data also showed that genes related to A-P pattern formation, regionalization, and pattern specification processes are enriched in the transcriptome of PGECs (Figure 1H). Given the success in hindgut lineage generation in CDX2$^+$ PGECs, we next

---

(C) Chromosomal karyotyping of original iPSC and iPSC-derived PGECs after 5 times of passaging.

(D) Maintenance of PGEC-related genes including *CDX2*, *SOX17*, *FOXA2*, and *c-KIT* at 5, 10, 15, and 20 times of passaging assessed by qRT-PCR (n = 3 independent experiments, mean ± SEM).

(E and F) Immunostaining analysis of pluripotency marker; NANOG and PGEC markers; CDX2, SOX17, FOXA2, and proliferation marker; Ki-67 in TKDA3-4-induced PGECs from different passage. Quantification data are shown in (F) (n = 3 independent experiments, mean ± SEM). Scale bar, 100 μm.

(G) Unsupervised hierarchical clustering using PGEC axis-contributing genes demonstrated that the feature of PGECs did not have relationship with the number of passage. The uncertainty of cluster was evaluated by bootstrapping, as shown in Supplemental Experimental Procedures.

(H) Number of mice bearing teratoma after transplanting iPSC or iPSC-derived PGECs.
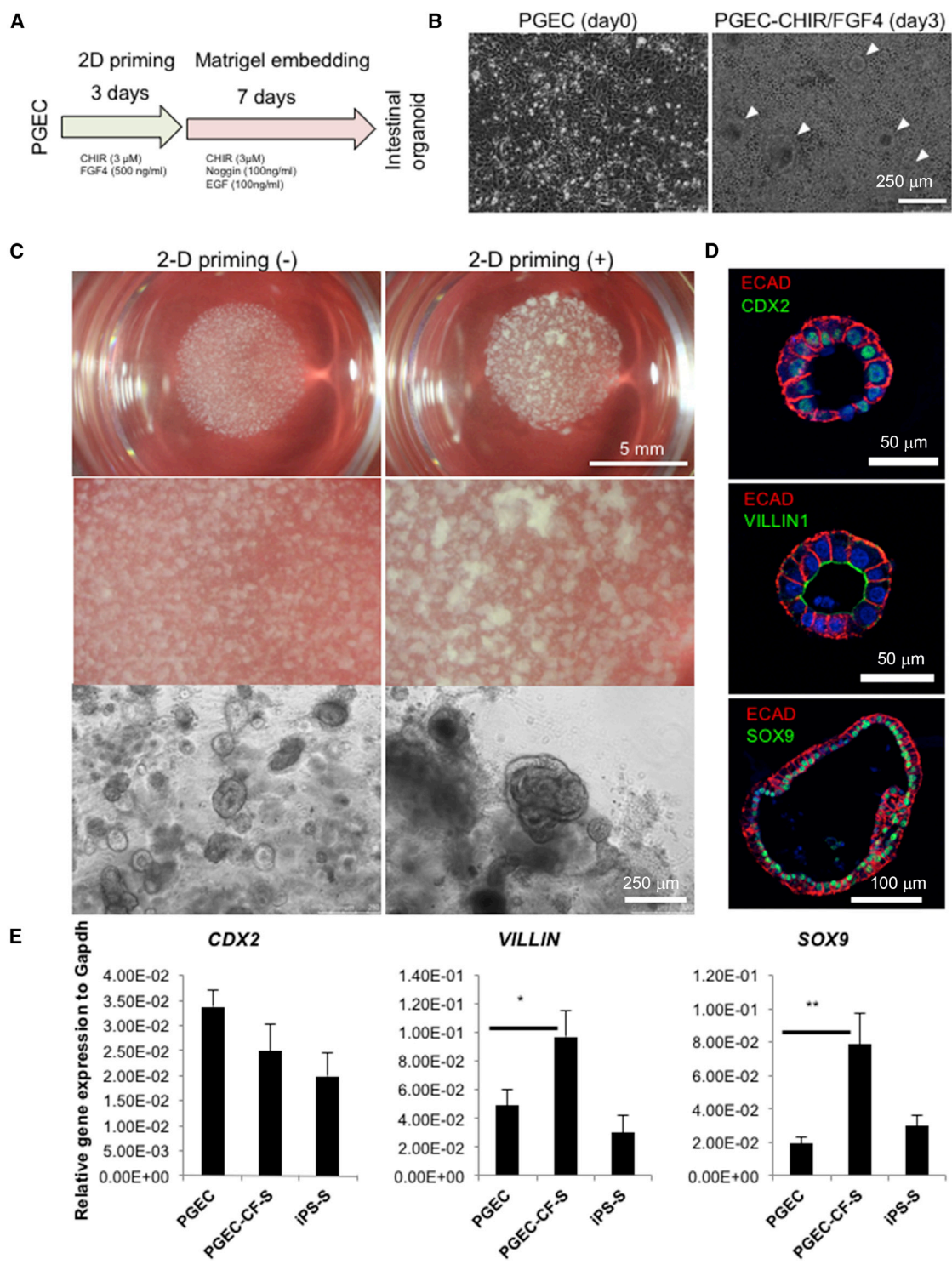
See also Figures S3–S5.

Figure 3. Hindgut Organoids from Posterior Gut Endoderm Cells

(A) The differentiation strategy of hindgut organoid generation from PGECs.

(B) Bright-field images of PGECs 2D cultured for 3 days in media with or without CHIR/FGF4. CHIR/FGF4 cultures drive three-dimensional spheroid generation (arrowheads). Scale bar, 250 μm.

tested whether the PGECs could be induced toward hepatic differentiation through our modified hepatic differentiation protocols. We found that both fresh and thawed PGECs could successfully differentiate into mature hepatocyte-like cells (PGEC-MHs) (Figure 4A). As determined by qRT-PCR (Figure 4B) and immunohistochemistry (Figure 4C), hepatic-related markers including *AFP*, *TTR*, *ALB*, *GLUT2*, *CK8*, *ZO-1*, and the liver-associated transcription factor *HNF4A* were induced in PGEC-MHs. Furthermore, microarray gene expression profiles indicated that PGEC-MHs showed signatures more similar to human adult hepatocytes or liver tissues, a result confirmed by pseudo-time and heatmap analyses of a previously reported hepatic developmental signature (Figure 4D).

PGEC-MHs exhibited glycogen accumulation by periodic acid-Schiff (PAS) staining, and these PAS-positive cells also showed a hepatocyte morphology (Figure 4E). The cellular uptake and excretion of indocyanine green (ICG) is a unique characteristic of hepatocytes, and cellular uptake was observed in a very high percentage of our PGEC-MHs. The excretion of ICG appeared 1 hr after the removal of ICG, with most of the ICG excreted within 3.5 hr (Figure 4E) and almost complete disappearance of the ICG by 12 hr. One of the important functions of hepatocytes is to secrete functioning proteins into the blood, such as albumin. An ELISA for human albumin showed that both fresh PGECs and thawed PGEC-derived mature hepatocytes secreted approximately $1{,}533 \pm 403$ ng/mL and $1{,}620 \pm 573$ ng/mL of albumin into the medium per million cells within 24 hr, which was significantly more than iPSC-derived mature hepatocytes (Figure 4F) ($p = 0.0003$, $n = 18$). Based on these analyses, we concluded that PGECs can efficiently and reproducibly generate hepatocyte-like cells under well-defined culture conditions.

PGEC-Derived Liver Bud Organoids Rescue an Acute Liver Failure Mouse Model

With our previous protocol for liver bud organoid generation, we cultured PGECs with endothelial (human umbilical vein endothelial cell [HUVEC]) and mesenchymal (mesenchymal stem cell [MSC]) lineages (Figure 5A) to generate PGEC liver bud organoids (PGEC-LBs). After co-culture, human PGECs self-organized into macroscopically visible 3D cell clusters with an intrinsic organizing capacity up to 72 hr after seeding (Figure 5B). To examine whether this protocol was appropriate for PGECs, we first analyzed the human albumin secretion between different culture media of hepatocytes and epithelial cell growth (HCM/EGM). After culture for 8 days, significantly higher human albumin secretion was detected under HCM/EGM culture conditions (427 ± 34 ng/mL and 552 ± 85 ng/mL, respectively) (Figure 5C). qPCR analysis further revealed the significantly increased expression of early hepatic marker genes such as *ALB*, *G6P*, *HNF4A* and *CYP3A7* by PGEC-LBs (Figure 5D). Another important indicator of hepatocyte function, ammonia removal, was also carried out and showed detoxifying ammonia capability in *in vitro* conditions (Figure 5E). Human serum albumin was tracked by ELISA under long-term culture of PGEC-LBs, and the results showed that human albumin was secreted into the culture media at approximately day 7, and up to $1{,}063 \pm 127$ ng/mL of human albumin was produced by day 28 of culture. Additionally there was a significantly higher human albumin concentration in the PGEC-LB group compared with the PGEC-only group (Figure 5F) ($p < 0.0001$, $n = 5$). To evaluate the functional maturation of human PGEC-LBs, we transplanted PGEC-LBs into an acute liver failure mouse model (*Alb*-TRECK/SCID) by kidney capsule transplantation. Notably, compared with the sham group, PGEC-LB transplantation significantly rescued mouse survival ($p = 0.036$) (Figure 5G). These results suggest that PGEC-LBs with a 3D and vascularized structure achieved successful engraftment and differentiation *in vivo*. The PGEC-LB-derived tissue exhibited hepatic cord-like structures (Figure 5H) at day 30, and immunohistochemistry showed positive detection of human nuclei, the vascular marker CD31, the bile duct marker CK19, and the mature hepatocyte marker human ALB (Figure 5H), suggesting the maturation of human PGEC-LBs *in vivo*.

DISCUSSION

Human Posterior Gut Endoderm with Foregut Potential: A Developmentally Relevant Population?

Soon after endoderm specification, the primitive gut is divided into regions with distinct gene expression patterns along the A-P axis. Wnt signaling is active in the posterior

---

(C) Macro- and bright-field images of 3D culture-derived hindgut organoids with or without 2D CHIR/FGF4 treatment. 2D priming with CHIR/FGF4 treatment formed highly convoluted epithelial structures. 2D priming: treatment with CHIR/FGF4 prior to 3D culture. Scale bars, 250 μm and 5 mm.

(D) Seven-day PGEC-derived organoid 3D cultures immunofluorescently analyzed for VILLIN and epithelial marker E-CADHERIN (ECAD), as well as hindgut transcription factor CDX2 and SOX9, identify polarized structure in PGEC-derived hindgut organoids. Nuclei were counterstained with DAPI (blue). Scale bars, 50 μm and 100 μm.

(E) qRT-PCR of *VILLIN* and *SOX9* suggests that PGEC differentiates into enterocyte lineage. PGEC-CF-S, PGEC-derived hindgut organoids with CHIR/FGF4 prior treatment; iPS-S, iPSC-derived hindgut organoids ($n = 3$ independent experiments, mean $\pm$ SEM; *$p < 0.05$, **$p < 0.01$).
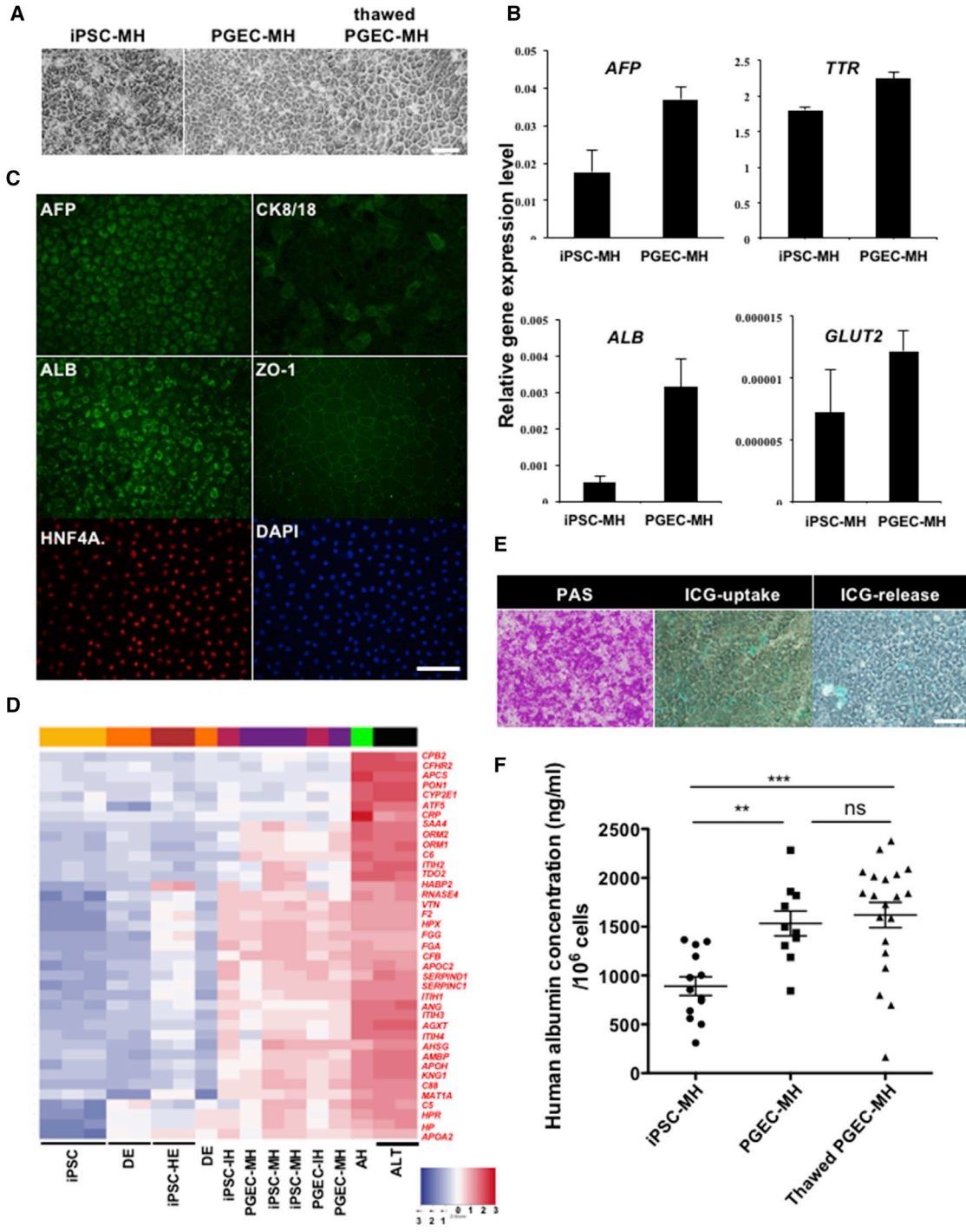
Figure 4. Unexpected Efficient Hepatic Differentiation of CDX2+ PGECs

(A) Bright-field images of mature hepatocyte (MH) morphology differentiated from iPSCs, PGECs, and thawed PGECs. Scale bar, 200 μm.

(B) qPCR analyzed the mRNA expression level of *AFP*, *TTR*, *ALB*, and *GLUT2* in iPSC- and PGEC-derived mature hepatocytes (MH) (n = 3 independent experiments, mean ± SEM).

(C) PGEC-derived mature hepatocytes were immunostained with various mature hepatocyte markers (AFP, CK8/18, ALB, ZO-1, and HNF4A); nuclei were counterstained with DAPI (blue). Scale bar, 200 μm.

(legend continued on next page)

endoderm as early as E7.5 to induce the intestinal master regulator *Cdx2*, shifting global gene expression toward a posteriorized intestinal program (Dye et al., 2015). *Cdx2* genes thus influence early A-P patterning all along the complete vertebral column and act as later mediators of posterior axial elongation (McCracken et al., 2014). Experiments in mice and *Xenopus* have suggested that *Cdx2* genes may be directly involved in the regulation of *Hox* genes, and a subset of the posterior enteric *Hox* code is dependent on the presence of *Cdx2*, which is indicative of a transcriptional network in the establishment of regional identity, especially in the posterior gut domain (Gao et al., 2009). The intestinal epithelium is constantly repopulated by the coordinated division of stem cells into faster cycling transit-amplifying cells that divide to produce all differentiated cells (Sheaffer and Kaestner, 2012).

However, among the extensive studies of *Cdx2*-positive PGECs and their functions in regional specification and morphogenesis of the intestine *in vivo*, no studies have shown whether *CDX2*-positive PGECs can be differentiated *in vitro* from human iPSCs with the extensive proliferation capability. Herein, by mimicking the molecular developmental mechanism in mice, we succeeded in inducing CDX2$^+$ cell populations from human iPSCs with EGF, VEGF, FGF2, Chir99021, and A83-01 treatment. Global gene analysis revealed that our generated CDX2$^+$ cells highly expressed the posterior *HOX* genes and actively functioned in A-P patterning formation and regionalization, indicating that the CDX2$^+$ PGECs could be differentiated from human iPSCs *in vitro*. Thus, PGECs possessed a posteriorized gut endoderm phenotype with clear CDX2 expression, efficiently contributing to midgut and hindgut lineages with an extensive elongation potential.

From an endoderm developmental biology perspective, one interesting highlight of our human PGEC analysis is the remarkable differentiation propensity toward foregut-derived cells. Even with the use of an expanded clone, CDX2$^+$ PGECs hold hepatic and hindgut lineages as well as a higher functionality than iPSCs for liver bud organoid formation. These results raise a question related to human developmental biology: does the CDX2$^+$ posteriorized human gut naturally give rise to a part of the foregut endoderm tissue? To answer this question, a careful study using early human embryos is necessary to determine whether CDX2$^+$ PGECs are developmentally relevant and capable of differentiating posterior foregut cells, revisiting the concept of early human endoderm development by defining the presence of CDX2$^+$ transitional posterior endoderm precursors.

Robust Amplification of Storable PGECs under Xeno- and Feeder-free Conditions

iPSC technology holds promise for regenerative medicine, disease modeling, and drug development. However, the current major limitation of this technology involves the establishment of approaches to obtain sufficient quantity and quality of cell sources for realistic medical applications because of the tumor-prone nature and, more importantly, the reproducibility challenges associated with the use of PSCs. Toward this aim, the derivation of lineage-committed expandable progenitors would be a rational approach to generate a stable supply for medical applications. Recent studies have shown the possibility of this concept in endoderm derivatives by differentiating or reprogramming multipotent endoderm progenitors (Cheng et al., 2012; Zhu et al., 2014) or foregut stem cells (Hannan et al., 2013), yet these cells relied on the use of feeders or xenogeneic products including serum, which are not compatible with clinical applications. In contrast, our CDX2$^+$ PGECs represent a more desirable approach to generate specific endodermal lineage cells because of their rigorous proliferative potential *in vitro* and the absence of teratoma formation *in vivo* with the use of chemically defined media under feeder-free conditions. As PGEC generation does not necessarily require Matrigel, the use of Laminin-511 E8 will alleviate safety concerns associated with PGEC generation for future clinical application. In fact, *in vitro* our PGECs displayed a 10^{21}-fold increase in cell number after more than 20 passages without any gene/viral transduction or feeder cell usage. Global gene analysis and chromosomal stability analysis revealed the proliferation and differentiation stability of PGECs based on gene and protein expression, presumably because these cells are inherently amenable to intensive proliferative stimuli that are experienced during development throughout the gut elongation process. Additionally, PGECs were successfully generated from five different iPSC lines. Given the necessity of 10^{10}-scale hepatocytes for therapeutic applications in

(D) Heatmap of gene array analyses showing that expression of 40 liver-specific mRNAs (Ma et al., 2013) was increased (red) in iPSC and PGEC-derived immature hepatocyte (IH) and mature hepatocyte (MH) compared with undifferentiated (iPSC, DE, HE) cells where the majority of these mRNAs were expressed at relatively low levels (blue). AH, adult hepatocytes; ALT, adult liver tissue.

(E) PAS assay of differentiated PGEC cells indicated numerous hepatocytes exhibiting cytoplasmic glycogen storage. Cellular uptake and excretion of indocyanine green (ICG) confirmed the metabolism of ICG. Scale bar, 200 μm.

(F) Albumin secretion by iPSC-, PGEC-, and thawed PGEC-derived mature hepatocytes was assayed by ELISA. The differentiation medium was changed to fresh medium 24 hr before the assay. This experiment suggested the highly efficient hepatocyte differentiation potential of PGEC compared with iPSC (n = 3 independent experiments, mean ± SEM; ns, no significant difference; **p < 0.01, ***p < 0.001).
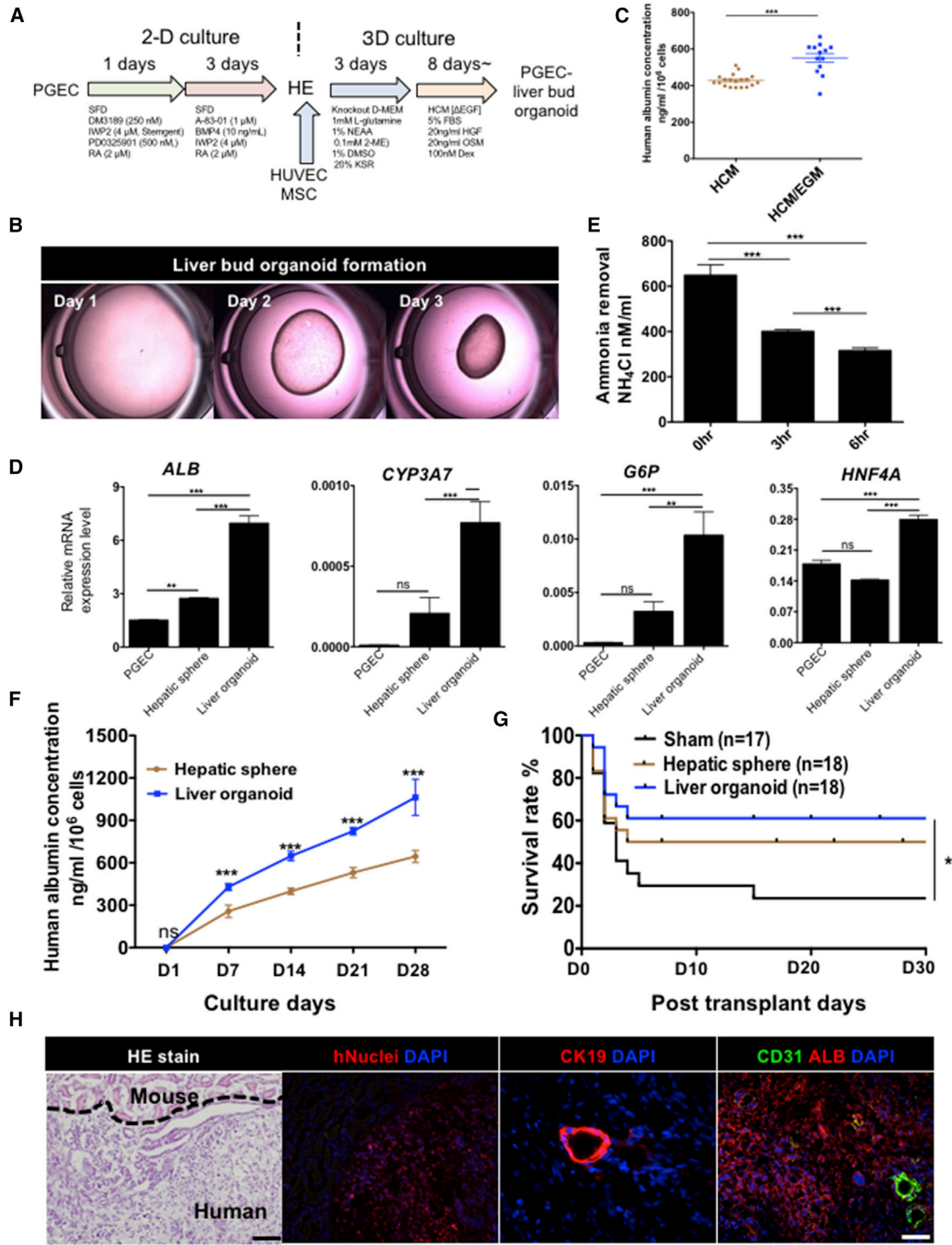
Figure 5. PGEC-Derived Liver Bud Organoid Transplant Rescue of Liver Failure

(A) Differentiation strategy of liver bud organoids (PGECs co-cultured with HUVEC and MSC) and hepatic sphere (PGECs only) from PGECs.

(B) Time-lapse imaging through liver bud organoid formation from PGECs.

(C) ELISA of PGEC-derived liver bud organoids secreted higher human albumin in medium HCM/EGM compared with HCM, suggests HCM/EGM (1:1) is the most efficient medium for PGEC-derived liver bud organoids toward hepatic differentiation (n = 3 independent experiments, mean ± SEM; ***p < 0.001).

(legend continued on next page)

adults, the use of storable and robustly amplifying PGECs from feeder-free human iPSCs represents a rational cell source for future applications.

Self-Organizing Liver Bud Organoid Generation Using PGECs Highlights Their Therapeutic Applications

Recent technological advancements in developing self-organizing organoids provide a new opportunity to study organogenesis and drug development. At present, a number of protocols for 3D organoid cultures have been established, including for the intestine (Dye et al., 2015; Spence et al., 2011), stomach (McCracken et al., 2014), optic cup (Eiraku et al., 2011; Nakano et al., 2012), optic vesicle (Koehler and Hashino, 2014), and cerebellum (Lancaster et al., 2013), using human PSCs. These organoid approaches not only hold promise for use in regenerative medicine but also may serve as novel platforms for disease modeling and drug development. In this context, we showed the successful adaptation of PGECs for liver bud organoid formation. Notably, our CDX2^{+} PGECs efficiently generated liver bud organoids after co-culture with endothelial and mesenchymal cells, and *in vivo* transplantation of PGEC-derived liver bud organoids rescued mouse survival from acute liver failure. These results indicate that CDX2^{+} PGECs may be promising candidates for *in vivo* modeling and autologous therapy for human liver diseases because PGECs *in vivo* bear characteristics of tumor resistance.

Finally, the derivation of PGECs is highly reproducible because PGEC differentiation was successful in all five of the tested iPSC lines without a need to establish extensively individualized protocols. Collectively, PGECs not only provide a unique *in vitro* model of human endoderm development but also represent an important tool to deliver the clinical or pharmaceutical promises of human iPSCs in medical applications.

EXPERIMENTAL PROCEDURES

Human iPSC Culture and Definitive Endoderm Cell Induction

Human iPSCs were routinely cultured in mTeSR1 on Matrigel (growth factor reduced) (BD Biosciences, Bedford, MA, USA)-coated plates for the TKDA3-4 iPSC clone and in StemFit (AK03N, Ajinomoto, Tokyo, Japan) on Laminin-511 E8 (Nippi, Tokyo, Japan)-coated dishes for the clinical xeno-free iPSC clones including D2, 1383D6, 1231A3, and Ff06. To generate definitive endoderm cells, we plated monolayers of pluripotent cells harvested using Accutase (Millipore, Billerica, MA, USA) on 6-well plates (Corning Costar #3516) (Corning, NY, USA) pre-coated with 1:30 diluted Matrigel (growth factor reduced; BD Bioscience) or $0.5\ \mu g/cm^2$ Laminin-511 E8 (Nippi) at a density of 6×10^5 cells per well with 100 ng/mL activin A (R&D Systems, Minneapolis, MN, USA), 50 ng/mL Wnt3a, and 10 μM Rock inhibitor Y27632 in RPMI/B27 (Invitrogen, Carlsbad, CA, USA) medium for 1 day. Differentiation was initiated by culture with 100 ng/mL activin A and 50 ng/mL Wnt3a in RPMI/B27 medium for 1 day under 5% CO_2, followed by 2 days with 100 ng/mL activin A, 0.5 ng/mL BMP4 (Peprotech, Rocky Hill, NJ, USA), 5 ng/mL FGF2 (Invitrogen), and 10 ng/mL VEGF (Gibco, Carlsbad, CA, USA) in RPMI/B27 under 5% CO_2, then followed by another 2 days with 100 ng/mL activin A, 0.5 ng/mL BMP4 (Peprotech), 5 ng/mL FGF2 (Invitrogen), and 10 ng/mL VEGF (Gibco) in SFD-based medium under 5% CO_2.

Establishment and Maintenance of Posterior Gut Endoderm Cells

The optimal culture conditions for maintaining PGECs were established by culturing cells on growth factor-reduced Matrigel (TKDA3-4 derived PGECs) or recombinant Laminin-511 E8 (1231A3-, 1383D2-, 1383D6-, and Ff06-derived PGECs) and promoting cell differentiation. This medium was composed of SFD-based medium supplemented with FGF2 (5 ng/mL), VEGF (10 ng/mL), EGF (20 ng/mL; Sigma, St. Louis, MO, USA), Chir99021 (3 μM; Peprotech), and A83-01 (0.5 μM; Tocris, Bristol, UK). SFD-based medium contained 75% IMDM (Invitrogen), 25% F12 nutrient medium (Invitrogen), monothioglycerol (4.5×10^{-4} M), 1% B27 (Invitrogen), 1% N2 supplement (Invitrogen), 50 μg/mL ascorbic acid (Sigma), 0.1% BSA (Sigma), and 1 mM L-glutamine (Invitrogen).

Differentiation of PGECs

For hepatic differentiation, PGECs were dissociated with Accutase and then replated onto Matrigel (1:30 dilution)- or Laminin 511 E8-coated 12-well tissue culture plates (BD) at 1×10^5 cells per well as adherent cultures. SFD-based medium was used for the first 4 days for hepatic differentiation of PGECs. During the first 4 days of differentiation, the following cytokines and growth factors were

---

(D) qRT-PCR analysis of hepatic markers (*ALB*, *HNF4A*, *CYP3A7*, and *G6P*) in PGEC-derived liver bud organoids (day 15), hepatic sphere (day 15), and original PGEC (n = 3 independent experiments, mean ± SEM; ns, no significant difference; **p < 0.01, ***p < 0.001).

(E) Ammonium removal capacity in PGEC liver organoids (day 15) (n = 3 independent experiments, mean ± SEM; ***p < 0.001).

(F) Human albumin secretion by hepatic sphere and liver bud organoids was assayed by ELISA. The differentiation medium was changed to fresh medium 24 hr before the assay. The amount of albumin released into the medium per 24 hr per 10^6 cells was measured at days 1, 7, 14, 21, and 28 of differentiation in HCM/EGM (n = 3 independent experiments, mean ± SEM; ns, no significant difference; ***p < 0.001).

(G) Survival curve of liver bud organoid-transplanted (n = 18), hepatic sphere-transplanted (n = 18), and sham-transplanted (n = 17) groups following lethal liver failure in *Alb*-TRECK-scid mouse. *p < 0.05.

(H) H&E staining and immunostaining (human nuclei, human CK19, human CD31, and human albumin) shows hepatic tissue formation from 30 days after liver bud organoids were transplanted into *Alb*-TRECK-scid mouse. Scale bar, 50 μm.

added: DM3189 (250 nM), IWP2 (4 μM; Stemgent), PD0325901 (500 nM), and RA (2 μM) for 1 day, followed by A-83-01 (1 μM), BMP4 (10 ng/mL), IWP2 (4 μM), and RA (2 μM) for another 3 days. For the next 3 days, cells were cultured in Knockout DMEM with 1 mM L-glutamine, 1% non-essential amino acids, 0.1 mM 2-mercaptoethanol, 1% DMSO, and 20% Knockout serum replacement (Gibco). From day 8 on, the medium contained hepatocyte growth factor (100 ng/mL), oncostatin M (20 ng/mL), and dexamethasone (2×10^{-7} M) in hepatocyte culture medium; the medium was changed every 2 days.

For hindgut differentiation of PGECs, a modification of the protocol described by Spence et al. (2011) was used. Cultured PGECs in 24-well plates were treated with Chir99021 (3 μM) and FGF4 (500 ng/mL) for 3 days and were then harvested by digesting the Matrigel with collagenase B treatment at 37°C for 1 hr. The resultant colonies were mixed with undiluted Matrigel (BD Biosciences) and were differentiated with DMEM/F12 advanced medium containing 1% penicillin/streptomycin, 2 mM L-glutamine, B27, 15 mM HEPES, 500 ng/mL R-spondin-1, 100 ng/mL Noggin, and 100 ng/mL EGF. Cells were fed every 2–3 days.

All the differentiation cultures of PGECs were maintained in a 5% CO_2/90% N_2 environment. All cytokines were purchased from R&D except for indicates. The protocols of human iPSC culture and transplantation into animals were approved by the relevant ethical committee of Yokohama City University.

Statistics

The statistical significance of differences was evaluated by the Mann-Whitney U test when two groups were compared or by one-way ANOVA and Bonferroni's multiple comparison tests when multiple groups were compared. We used the log-rank (Mantel-Cox) test and Kaplan-Meier method to assess post-transplantation survival. A p value of less than 0.05 was considered statistically significant, Statistical analysis was performed using GraphPad Prism. Additional experimental procedures are listed in Supplemental Experimental Procedures.

ACCESSION NUMBERS

Gene expression data are publicly available and can be retrieved from the GEO, NCBI under accession number GEO: GSE108937.

SUPPLEMENTAL INFORMATION

Supplemental Information includes Supplemental Experimental Procedures, five figures, and three tables and can be found with this article online at https://doi.org/10.1016/j.stemcr.2018.01.006.

AUTHOR CONTRIBUTIONS

R.-R.Z. performed experiments, analyzed data, and prepared the manuscript. T. Takebe designed, supervised, and performed experiments, analyzed data, and prepared the manuscript. M.K. and Y.U. performed the microarray experiment and informatics analysis. T.M., R.O., and T. Tadokoro performed experiments and analyzed data for the hindgut differentiation. T. Takebe, K.S., and H.T. provided critical discussions.

REFERENCES

Cang, Y., Zhang, J., Nicholas, S.A., Kim, A.L., Zhou, P., and Goff, S.P. (2007). DDB1 is essential for genomic stability in developing epidermis. Proc. Natl. Acad. Sci. USA 104, 2733–2737.

Cervantes, S., Yamaguchi, T.P., and Hebrok, M. (2009). Wnt5a is essential for intestinal elongation in mice. Dev. Biol. 326, 285–294.

Chawengsaksophak, K., de Graaff, W., Rossant, J., Deschamps, J., and Beck, F. (2004). Cdx2 is essential for axial elongation in mouse development. Proc. Natl. Acad. Sci. USA 101, 7641–7645.

Cheng, X., Ying, L., Lu, L., Galvão, A.M., Mills, J.A., Lin, H.C., Kotton, D.N., Shen, S.S., Nostro, M.C., and Choi, J.K. (2012). Self-renewing endodermal progenitor lines generated from human pluripotent stem cells. Cell Stem Cell 10, 371–384.

Christoforou, N., Liau, B., Chakraborty, S., Chellapan, M., Bursac, N., and Leong, K.W. (2013). Induced pluripotent stem cell-derived cardiac progenitors differentiate to cardiomyocytes and form biosynthetic tissues. PLoS One 8, e65963.

Date, S., and Sato, T. (2015). Mini-gut organoids: reconstitution of the stem cell niche. Annu. Rev. Cell Dev. Biol. 31, 269–289.

Dye, B.R., Hill, D.R., Ferguson, M.A., Tsai, Y.-H., Nagy, M.S., Dyal, R., Wells, J.M., Mayhew, C.N., Nattiv, R., and Klein, O.D. (2015). In vitro generation of human pluripotent stem cell derived lung organoids. Elife 4, e05098.

Eiraku, M., Takata, N., Ishibashi, H., Kawada, M., Sakakura, E., Okuda, S., Sekiguchi, K., Adachi, T., and Sasai, Y. (2011). Self-organizing optic-cup morphogenesis in three-dimensional culture. Nature 472, 51–56.

Elliott, E.N., Sheaffer, K.L., Schug, J., Stappenbeck, T.S., and Kaestner, K.H. (2015). Dnmt1 is essential to maintain progenitors in the perinatal intestinal epithelium. Development 142, 2163–2172.

Franklin, V., Khoo, P.L., Bildsoe, H., Wong, N., Lewis, S., and Tam, P.P. (2008). Regionalisation of the endoderm progenitors and morphogenesis of the gut portals of the mouse embryo. Mech. Dev. 125, 587–600.

Gadue, P., French, D., and Cheng, X. (2013). Self-renewing endodermal progenitor lines generated from human pluripotent stem cells and methods of use thereof (Google Patents).

Gao, N., White, P., and Kaestner, K.H. (2009). Establishment of intestinal identity and epithelial-mesenchymal signaling by Cdx2. Dev. Cell 16, 588–599.

Gouon-Evans, V., Boussemart, L., Gadue, P., Nierhoff, D., Koehler, C.I., Kubo, A., Shafritz, D.A., and Keller, G. (2006). BMP-4 is required for hepatic specification of mouse embryonic stem cell-derived definitive endoderm. Nat. Biotechnol. 24, 1402–1411.

Gregorieff, A., and Clevers, H. (2005). Wnt signaling in the intestinal epithelium: from endoderm to cancer. Genes Dev. 19, 877–890.

Hagedorn, C., Blanch, A.R., and Harwood, V.J. (2011). Microbial Source Tracking: Methods, Applications, and Case Studies (Springer Science & Business Media).

Hannan, N.R., Fordham, R.P., Syed, Y.A., Moignard, V., Berry, A., Bautista, R., Hanley, N.A., Jensen, K.B., and Vallier, L. (2013). Generation of multipotent foregut stem cells from human pluripotent stem cells. Stem Cell Rep. 1, 293–306.

Hu, B.-Y., Weick, J.P., Yu, J., Ma, L.-X., Zhang, X.-Q., Thomson, J.A., and Zhang, S.-C. (2010). Neural differentiation of human induced pluripotent stem cells follows developmental principles but with variable potency. Proc. Natl. Acad. Sci. USA 107, 4335–4340.

Ikonomou, L., and Kotton, D.N. (2015). Derivation of endodermal progenitors from pluripotent stem cells. J. Cell. Physiol. 230, 246–258.

Koehler, K.R., and Hashino, E. (2014). 3D mouse embryonic stem cell culture for generating inner ear organoids. Nat. Protoc. 9, 1229–1244.

Lancaster, M.A., Renner, M., Martin, C.A., Wenzel, D., Bicknell, L.S., Hurles, M.E., Homfray, T., Penninger, J.M., Jackson, A.P., and Knoblich, J.A. (2013). Cerebral organoids model human brain development and microcephaly. Nature 501, 373–379.

Lund, R.J., Närvä, E., and Lahesmaa, R. (2012). Genetic and epigenetic stability of human pluripotent stem cells. Nat. Rev. Genet. 13, 732–744.

Ma, X., Duan, Y., Tschudy-Seney, B., Roll, G., Behbahan, I.S., Ahuja, T.P., Tolstikov, V., Wang, C., McGee, J., and Khoobyari, S. (2013). Highly efficient differentiation of functional hepatocytes from human induced pluripotent stem cells. Stem Cells Transl. Med. 2, 409–419.

McCracken, K.W., Catá, E.M., Crawford, C.M., Sinagoga, K.L., Schumacher, M., Rockich, B.E., Tsai, Y.-H., Mayhew, C.N., Spence, J.R., and Zavros, Y. (2014). Modelling human development and disease in pluripotent stem-cell-derived gastric organoids. Nature 516, 400–404.

Nakano, T., Ando, S., Takata, N., Kawada, M., Muguruma, K., Sekiguchi, K., Saito, K., Yonemura, S., Eiraku, M., and Sasai, Y. (2012).

Self-formation of optic cups and storable stratified neural retina from human ESCs. Cell Stem Cell 10, 771–785.

Peterson, S.E., and Loring, J.F. (2014). Genomic instability in pluripotent stem cells: implications for clinical applications. J. Biol. Chem. 289, 4578–4584.

Reynolds, A., Wharton, N., Parris, A., Mitchell, E., Sobolewski, A., Kam, C., Bigwood, L., El Hadi, A., Münsterberg, A., and Lewis, M. (2014). Canonical Wnt signals combined with suppressed TGFβ/BMP pathways promote renewal of the native human colonic epithelium. Gut 63, 610–621.

Sato, T., and Clevers, H. (2013). Growing self-organizing mini-guts from a single intestinal stem cell: mechanism and applications. Science 340, 1190–1194.

Sheaffer, K.L., and Kaestner, K.H. (2012). Transcriptional networks in liver and intestinal development. Cold Spring Harb. Perspect. Biol. 4, a008284.

Sherwood, R.I., Chen, T.Y.A., and Melton, D.A. (2009). Transcriptional dynamics of endodermal organ formation. Dev. Dyn. 238, 29–42.

Sherwood, R.I., Maehr, R., Mazzoni, E.O., and Melton, D.A. (2011). Wnt signaling specifies and patterns intestinal endoderm. Mech. Dev. 128, 387–400.

Shi, W., Bain, A.L., Schwer, B., Al-Ejeh, F., Smith, C., Wong, L., Chai, H., Miranda, M.S., Ho, U., Kawaguchi, M., et al. (2013). Essential developmental, genomic stability, and tumour suppressor functions of the mouse orthologue of hSSB1/NABP2. PLoS Genet. 9, e1003298.

Shi, Y., Kirwan, P., Smith, J., Robinson, H.P., and Livesey, F.J. (2012). Human cerebral cortex development from pluripotent stem cells to functional excitatory synapses. Nat. Neurosci. 15, 477–486.

Silberg, D.G., Sullivan, J., Kang, E., Swain, G.P., Moffett, J., Sund, N.J., Sackett, S.D., and Kaestner, K.H. (2002). Cdx2 ectopic expression induces gastric intestinal metaplasia in transgenic mice. Gastroenterology 122, 689–696.

Spence, J.R., Mayhew, C.N., Rankin, S.A., Kuhar, M.F., Vallance, J.E., Tolle, K., Hoskins, E.E., Kalinichenko, V.V., Wells, S.I., and Zorn, A.M. (2011). Directed differentiation of human pluripotent stem cells into intestinal tissue in vitro. Nature 470, 105–109.

Tortora, G.J., and Derrickson, B.H. (2008). Principles of Anatomy and Physiology (John Wiley & Sons).

Wang, W.E., Chen, X., Houser, S.R., and Zeng, C. (2013). Potential of cardiac stem/progenitor cells and induced pluripotent stem cells for cardiac repair in ischaemic heart disease. Clin. Sci. 125, 319–327.

Wells, J.M., and Melton, D.A. (1999). Vertebrate endoderm development. Annu. Rev. Cell Dev. Biol. 15, 393–410.

Zhu, S., Rezvani, M., Harbell, J., Mattis, A.N., Wolfe, A.R., Benet, L.Z., Willenbring, H., and Ding, S. (2014). Mouse liver repopulation with hepatocytes generated from human fibroblasts. Nature 508, 93–97.

Zorn, A.M., and Wells, J.M. (2009). Vertebrate endoderm development and organ formation. Annu. Rev. Cell Dev. Biol. 25, 221–251.